MECHANICS OF FRP SHEAR STRENGTHENING OF RC BEAMS

G. Monti, F. Santinelli and M. A. Liotta

Dipartimento di Ingegneria Strutturale e Geotecnica, Università di Roma La Sapienza, Roma, Italy

ABSTRACT

This paper presents the results of an experimental/analytical study aiming at obtaining a clear understanding of the underlying mechanisms of the shear strengthening of reinforced concrete beams with fibre reinforced polymers (FRP). Through the definition of the generalised constitutive law of a bonded FRP sheet, of the compatibility imposed by the shear crack opening, and of the appropriate boundary conditions depending on the strengthening configuration, analytical expressions of the stress field in the FRP sheet crossing a shear crack are obtained. These expressions allow to easily define closed-form equations for the effective strength of FRP strips/sheets used for shear strengthening, as function of both the adopted strengthening configuration and some basic geometric and mechanical parameters. The FRP contribution is then added to those of concrete and steel, adequately weighed. The equations accuracy has been verified through correlation studies with experimental results obtained from the literature and from laboratory tests on purposely under-designed real-scale beam specimens, strengthened with different FRP schemes.

1. INTRODUCTION

In the development of practical and reliable design equations for shear strengthening of reinforced concrete elements with FRP composite materials, three aspects still remain not perfectly understood. The first regards the shear resisting mechanism that develops when FRP strips/sheets are side bonded, rather than U-jacketed or wrapped, to the element; in this case, a different mechanism than the Moersch truss activates, that is, a "crack-bridging" mechanism, similar in nature to those of aggregate interlock, dowel effect and concrete tooth. The second aspect regards the evaluation of the contribution of the FRP transverse strengthening to the shear capacity; as opposed to the case of steel transverse reinforcement, which is always considered as yielded, FRP is instead subjected to a variable tensile stress along the crack profile, which is usually expressed as an effective stress. The third aspect regards the evaluation of the relative contributions to the shear capacity of concrete, steel and FRP at ultimate; it is not guaranteed that both concrete and stirrups can exploit their maximum strength when in the presence of FRP strengthening. These aspects are the object of the present work, where they are treated from both the experimental and the analytical standpoint.

2. EXPERIMENTAL TESTS

Thirteen beam specimens, purposely designed as under-reinforced in shear, were tested with a 3-point bending scheme (Monti et al. 2004). The concrete mean compressive cubic strength was R_{cm} = 13.3 MPa and the steel rebars had mean yield strength f_{ym} = 500 MPa. The geometric dimensions of the beams were (Figure 1): span 2.80 m, cross-section width 250 mm and depth 450 mm. The longitudinal reinforcement was made of 4ϕ20 bottom and of 2ϕ20 top, while shear stirrups ϕ8/400 mm were used. In view of the external strengthening application the bottom corners of the beam were rounded with 30 mm radius. The nomenclature used for each typology is represented in Table 1.

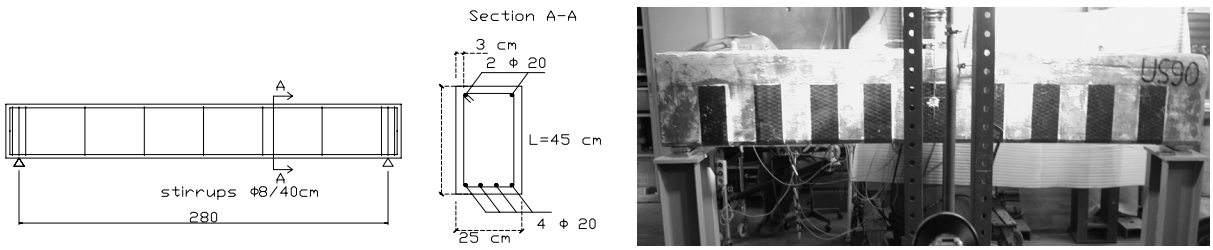

Figure 1. Reference specimen dimensions (left) and representative picture of a test (right).

Table 1. Typology, nomenclature and experimental shear strength of the tested beams.

STRENGTH'G APPLICATION	STRENGTH'G TYPE	FIBRES ANGLE	NAME	STRENGTHENING CONFIGURATION	EXP. SHEAR STRENGTH (kN)
	NONE	-	REF		95.0
SIDE BONDING	STRIPS width 150 mm spacing 300 mm	90°	SS90*		100.0
		45°	SS45		101.0
		60°, 45°, 30°	SSVA		105.0
	SHEETS	90°	SF90		112.5
U-JACKETING	STRIPS width 150 mm spacing 300 mm	90°	US90*		95.0
		60°	US60		111.0
		60°, 45°, 30°	USVA		120.0
		60°, 45°, 30°	USVA+		135.0
		45°	US45+		126.0
		90°	US90(2)*		90.0
	SHEETS	90°	UF90		125.0

* In these tests, the shear cracks did not fully activated the FRP strips, which then did not contribute to the shear strength.
All strips/sheets were in a single layer of CFRP, having thickness 0.22 mm and elastic modulus E_f = 390 GPa.

3. MECHANICS OF FRP SHEAR STRENGTHENING

In this section a coherent analytical framework to describe the behaviour of RC elements FRP-strengthened in shear is proposed, following previous efforts made by other authors (Täljsten 1997, Triantafillou 1998, Khalifa et al. 1998). The developed theory aims at producing closed-form expressions to describe the FRP stress distribution $\sigma_{f,cr}(x)$ along a shear crack (as qualitatively sketched in Figure 2), as opposed to regression-based formulas (*e.g.*, Triantafillou and Antonopoulos 2000). Once this is correctly defined, the FRP resultant across the crack can be computed and the FRP contribution to the resisting shear be found.

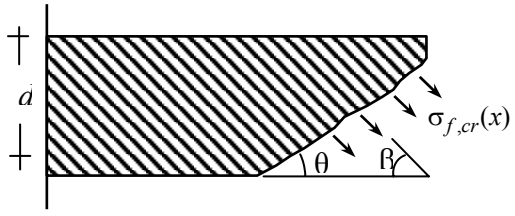

Figure 2. Stress distribution along an FRP sheet crossing a shear crack, from (*fib* 2001).

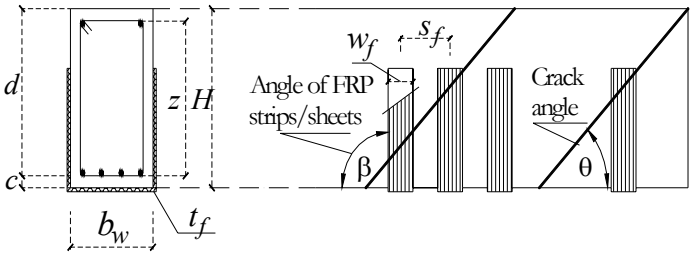

Figure 3. Geometry notation.

In the following developments, the following hypotheses are made (notation in Figure 3):

- Shear cracks are evenly spaced along the beam axis, and inclined with angle θ,
- At the ULS the cracks depth is equal to the internal lever arm $z = 0.9\,d$,
- In the case of U-jacketing (U) and wrapping (W), the resisting shear mechanism is based on the Moersch truss, while in the case of side bonding (S), because the Moersch truss cannot form as the tensile diagonal tie is missing, a different resisting mechanism of "crack-bridging" is considered to develop.

3.1 Generalised failure criterion of an FRP strip/sheet bonded to concrete

The criterion includes the two cases of: a) straight strip/sheet, and b) strip/sheet wrapped around a corner. Two quantities are introduced: the *effective bond length* L_e and the *debonding strength* $f_{fdd}(L)$, expressed as function of the available bond length L.
The effective bond length is given as (*e.g.*, Monti et al. 2003):

$$L_e = 0.6\sqrt{\frac{E_f \cdot t_f}{\sqrt{f_{ctm} \cdot k_b}}} \quad \text{(units: N, mm)} \tag{1}$$

where: E_f = FRP sheet elastic modulus, t_f = sheet thickness, $\tau_{max} = 1.8 \cdot f_{ctm} \cdot k_b$ = maximum bond strength (Brosens and Van Gemert 1999), where $f_{ctm} = 0.27 \cdot R_{ck}^{2/3}$ = concrete mean tensile strength (with R_{ck} = concrete characteristic cubic strength), and k_b = covering/scale coefficient (Brosens and Van Gemert 1999), given as:

$$k_b = \begin{cases} \sqrt{\dfrac{1.5}{1 + w_f/100 \text{ mm}}} & \text{for sheets} \\ \sqrt{\dfrac{1.5 \cdot (2 - w_f/s_f)}{1 + w_f/100 \text{ mm}}} & \text{for strips} \end{cases} \tag{2}$$

where, for strips: w_f = width measured orthogonally to β, s_f = spacing measured orthogonally to β; for sheets $w_f = \min(0.9d, h_w) \cdot \sin(\theta+\beta)/\sin\theta$, with d = beam effective depth, h_w = beam web depth, β = angle of strip/sheet to the beam axis, θ = crack angle to the beam axis.
The debonding strength is given as:

$$f_{fdd}(L) = \beta(L) \cdot f_{fdd} \tag{3}$$

where (Teng et al. 2002):

$$\beta(L) = \begin{cases} \sin\left(\dfrac{\pi}{2} \cdot \dfrac{L}{L_e}\right) & \text{for } L < L_e \\ 1 & \text{for } L \geq L_e \end{cases} \tag{4}$$

and (*e.g.*, Monti et al. 2003):

$$f_{fdd} = \sqrt{0.6\frac{E_f f_{ctm} k_b}{t_f}} \quad \text{(units: N, mm)} \tag{5}$$

The ultimate strength of the FRP strip/sheet, which includes the case when it is wrapped around a corner rounded with a radius R, is:

$$f_{fu}(L, \delta_e, R) = f_{fdd}(L) + \left\langle \eta_R \cdot f_{fu} - f_{fdd}(L) \right\rangle \cdot \delta_e, \quad \text{where: } \delta_e = \begin{cases} 0 & \text{free end} \\ 1 & \text{end around a corner} \end{cases} \tag{6}$$

where $\langle \cdot \rangle$ denotes that the content is zero if negative. It is noted that the sheet wrapped around a corner attains a fraction η_R of the ultimate strength f_{fu} of the FRP sheet depending on the coefficient η_R as function of the rounding radius R with respect to the beam width b_w (Campione and Miraglia 2003):

$$\eta_R = 0.2 + 1.6\frac{R}{b_w} \qquad 0 \leq \frac{R}{b_w} \leq 0.5 \tag{7}$$

When $L \geq L_e$, the expression for the ultimate strength of the FRP strip/sheet, wrapped around a corner with a radius R, becomes:

$$f_{fu,W}(R) = f_{fdd} + \left\langle \eta_R \cdot f_{fu} - f_{fdd} \right\rangle \tag{8}$$

3.2 **Generalised stress-slip constitutive law**

The generalised stress-slip law of FRP strips/sheets bonded to concrete, including both cases of free end or wrapped around a corner, is given as (symbols are shown in Figure 4):

$$\sigma_f(u,L,\delta_e)=\begin{cases} f_{fdd}\cdot\sin\left(\dfrac{\pi}{2}\cdot\dfrac{u}{u_1}\right) & \text{if} \quad u<u_1(L) \\ f_{fdd} & \text{if} \quad u_1(L)\le u<u_d(L) \\ f_{fdd}\cdot\left(\cos\left(\dfrac{u-u_d}{u_1}\cdot\dfrac{\pi}{2}\cdot(1-\delta_e)\right)\right) & \text{if} \quad u_d(L)\le u<u_u(L,\delta_e) \\ f_{fdd}\cdot\delta_e+\dfrac{E_f}{L}\cdot(u-u_u) & \text{if} \quad u_u(L,\delta_e)\le u<u_f(L,\delta_e,R) \\ 0 & \text{if} \quad u_f(L,\delta_e,R)\le u \end{cases} \tag{9}$$

Phase 1 in Figure 4: $u_1(L) = \min\{ u_1 L/L_e , u_1\}$ is the pulled end slip at the onset of debonding at the pulled end, as function of the available bond length L (up to either the free end or the corner rounding), where u_1 is (Brosens and Van Gemert 1999):

$$u_1 = 1.1\cdot k_b\cdot c_4 \text{ , with } c_4 = 0.3\,\text{mm} \tag{10}$$

Phase 2 in Figure 4: $u_d(L) = u_1(L) + \varepsilon_{fdd}\cdot\langle L - L_e\rangle$ is the pulled end slip at complete debonding over the length $L - L_e$, where $\varepsilon_{fdd} = f_{fdd} / E_f$ = strain in the straight portion up to the corner rounding and where $\langle\cdot\rangle$ denotes that the content is zero if negative.

Phase 3 in Figure 4: $u_u(L) = u_d(L) + u_1(L)$ = slip at complete debonding of the strip/sheet over the entire length L (the strip/sheet can go beyond this slip only if wrapped around a corner).

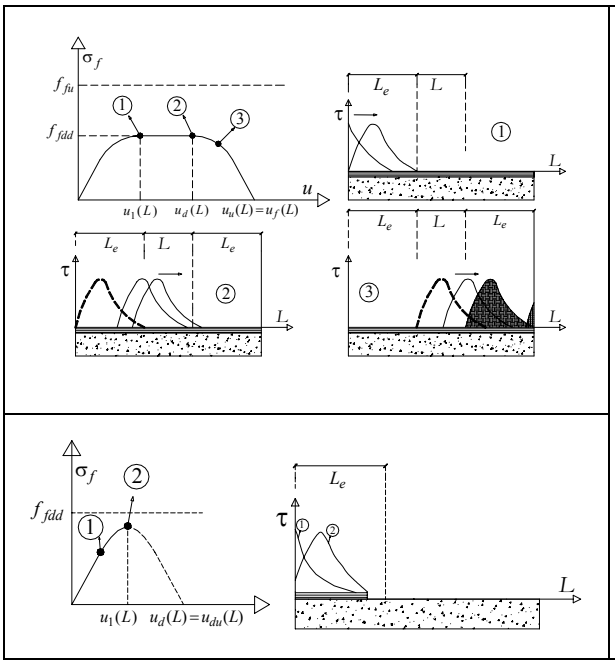

Figure 4. Stress-slip law for the case of FRP strip/sheet with free end and with sufficient bond length (Top), and with small bond length (Bottom).

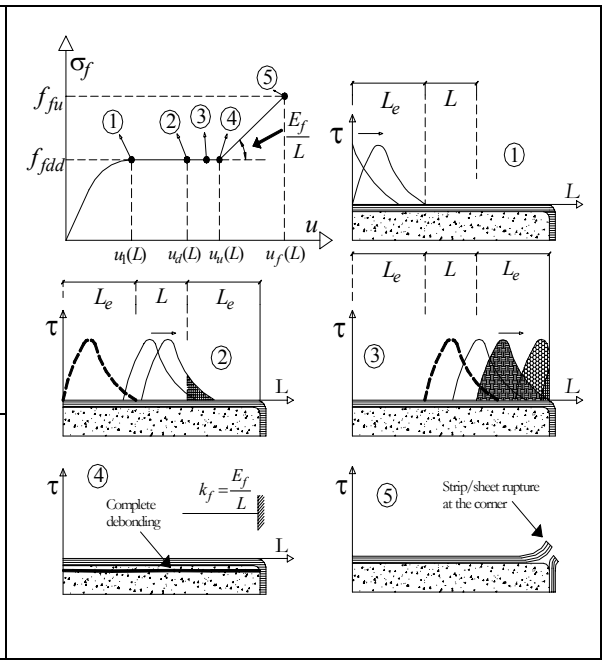

Figure 5. Stress-slip law for the case of FRP strip/sheet wrapped around a corner.

Phase 4-5 in Figure 5: when total debonding has occurred, the strip/sheet behaves as a pulled truss of stiffness L/E_f up to the ultimate strength, attained at the slip: $u_f\,(L,\delta_e,R) = u_u(L) + \langle f_{fu}(L,\delta_e,R) - f_{fdd}(L)\rangle\cdot L/E_f$, where it should be noticed that for strip/sheet with free end (with $\delta_e = 0$, and therefore with $f_{fu}(L,\delta_e,R) = f_{fdd}(L)$), it is: $u_f\,(L,\delta_e,R) = u_u(L)$.

The generalised stress-slip constitutive law also includes the particular (and rare) case of free end with $L<L_e$ (Figure 4, bottom).

3.3 **Compatibility (crack width)**

Considering a reference system with the origin fixed at the upper limit of the shear crack and with abscissa x along the crack itself (Figure 6), the crack width (normal to the crack axis) along the shear crack can be expressed as $w = w(x)$. In the following developments, in order to arrive at closed-form equations, a linear expression is used for the crack width:

$$w(x) = \alpha \cdot x \tag{11}$$

where α denotes the crack opening. Under the hypothesis of symmetric behaviour at the opposite sides of the crack, a slip is thus imposed to the strip/sheet crossing it, according to:

$$u(\alpha, x) = \frac{w(x)}{2} \cdot \sin(\theta + \beta) = \frac{1}{2}\alpha \cdot x \cdot \sin(\theta + \beta) \tag{12}$$

3.4 **Boundary conditions (available bond length)**

The boundary conditions refer to the available bond length $L(x)$ on both sides of the shear crack and should be defined according to the strengthening scheme adopted:

$$L(x) = \begin{Bmatrix} \min\{ L_{top}(x), L_{bot}(x) \} & \text{S} = \text{Side bonding} \\ L_{top}(x) & \text{U} = \text{U - jacketing} \\ \max\{ L_{top}(x), L_{bot}(x) \} & \text{W} = \text{Wrapping} \end{Bmatrix} \tag{13}$$

where: $L_{top}(x)$, $L_{bot}(x)$ = available bond lengths, starting from the crack axis towards the strip/sheet top and bottom end, respectively. Also, the strip/sheet end constraint is: $\delta_e = 0$ for S-strengthening and U-strengthening, and $\delta_e = 1$ for W-strengthening.
For case S (side bonding, Figure 6) one has:

$$L(x) = L_S(x) = \begin{cases} x \cdot \dfrac{\sin\theta}{\sin\beta} & \text{for} \quad 0 \le x < \dfrac{z}{2\sin\theta} \\ \dfrac{z}{\sin\beta} - x \cdot \dfrac{\sin\theta}{\sin\beta} & \text{for} \quad \dfrac{z}{2\sin\theta} \le x \le \dfrac{z}{\sin\theta} \end{cases} \tag{14}$$

For case U (U-jacketing, Figure 6) one has:

$$L(x) = L_U(x) = x \cdot \frac{\sin\theta}{\sin\beta} \quad \text{for} \quad 0 \le x \le \frac{z}{\sin\theta} \tag{15}$$

For case W (wrapping, Figure 6) one has:

$$L(x) = L_W(x) = \begin{cases} \dfrac{z}{\sin\beta} - x \cdot \dfrac{\sin\theta}{\sin\beta} & \text{for} \quad 0 \le x < \dfrac{z}{2\sin\theta} \\ x \cdot \dfrac{\sin\theta}{\sin\beta} & \text{for} \quad \dfrac{z}{2\sin\theta} \le x \le \dfrac{z}{\sin\theta} \end{cases} \tag{16}$$

and, for case W, it should be also noticed that, when the strip/sheet is completely debonded, it is still restrained at the two opposite wrapped ends, thus one has:

$$L(x) = \overline{L}_W(x) = \frac{z}{\sin\beta} \quad \text{for} \quad 0 \le x < \frac{z}{\sin\theta} \tag{17}$$

Considering the expression of the debonding strength (3), it is important to notice that there are zones with $L(x) < L_e$ where the debonding strength is not attained (and where one has $f_{fdd}[L(x)] < f_{fdd}$), and zones with $L(x) \ge L_e$, where the full debonding strength is attained.

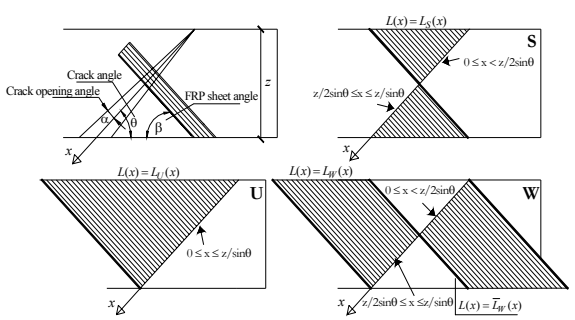

Figure 6. Boundary conditions (available bond length) for three strengthening configurations: S = Side bonding, U = U-jacketing, and W = Wrapping.

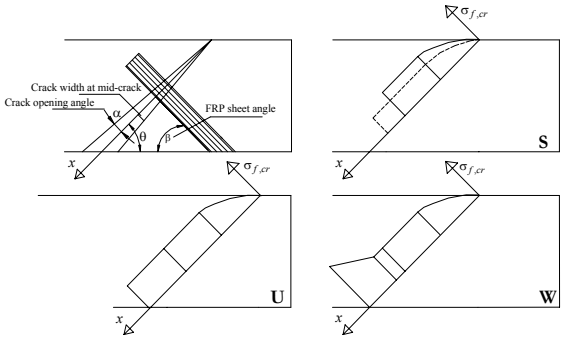

Figure 7. Typical stress profiles in FRP sheets along the shear crack for three strengthening configurations: S = Side bonding, U = U-jacketing, and W = Wrapping.

3.5 **FRP stress profile along the shear crack**

In order to obtain the stress profile in the FRP sheet along the crack as a function of both the crack opening and the available bond length on both sides of the crack itself, one has to substitute into the constitutive law $\sigma_f(u,L,\delta_e)$ of (9): a) the compatibility equation $u = u(\alpha,x)$ given by (12), b) the boundary condition $L = L(x)$ given either by (14) for Side Bonding or by (15) for U-jacketing or by (16) and (17) for Wrapping, and c) the end constraint given by the appropriate value of δ_e. Thus, it is obtained:

$$\sigma_{f,cr}[u(\alpha,x),L(x),\delta_e] =$$

$$= \begin{cases} f_{fdd}\cdot\sin\left(\dfrac{\pi}{2}\cdot\dfrac{u}{u_1}\right) & \text{if} \quad u < u_{1,cr}(L(x)) \\ f_{fdd} & \text{if} \quad u_{1,cr}(L(x)) \le u < u_{d,cr}(L(x)) \\ f_{fdd}\cdot\left(\cos\cdot\left(\dfrac{u-u_d}{u_1}\cdot\dfrac{\pi}{2}\cdot(1-\delta_e)\right)\right) & \text{if} \quad u_{d,cr}(L(x)) \le u < u_{u,cr}(L(x),\delta_e) \\ f_{fdd}\cdot\delta_e + \dfrac{E_f}{L}\cdot(u-u_u) & \text{if} \quad u_{u,cr}(L(x),\delta_e) \le u < u_{f,cr}(L(x),\delta_e,R) \\ 0 & \text{if} \quad u_{f,cr}(L(x),\delta_e,R) \le u \end{cases} \tag{18}$$

where the slips are: $u_{1,cr}[L(x)] = \min\{u_1 L(x)/L_e, u_1\}$, $u_{d,cr}[L(x)] = u_1 + \varepsilon_{fdd}\cdot\langle L(x) - L_e\rangle$, $u_{f,cr}[L(x)] = u_{u,cr}[L(x)] + \langle f_{fu}[L_e,\delta_e,R] - f_{fdd}[L_e]\rangle\cdot L_W(x)/E_f$, and especially:

$$u_{u,cr}[L(x)] = u_{d,cr}[L(x)] + u_{1,cr}[L(x)] \tag{19}$$

Figure 7 qualitatively depicts the $\sigma_{f,cr}(x)$ profiles along the crack as given by (18), for the three different strengthening configurations considered, when sheets are used. In the configuration S, the stress profile is truncated towards the end of the crack, where the available length tends to zero. In the configuration U, the stress profile remains constant where the available length allows the full debonding strength to be developed throughout the crack length. In the configuration W, the stress profile rises towards the end of the crack, where, after complete debonding, the sheet is restrained at both ends and subjected to simple tension up to its tensile strength.

3.6 **Determination of FRP contribution to the shear strength**

The objective is to obtain the maximum contribution of the FRP strips/sheet to the shear strength. This means to identify, among all possible shapes of the FRP stress profile $\sigma_{f,cr}[u(\alpha,x),L(x)]$, which changes with the crack opening α, the one offering the maximum contribution.

3.6.1 *Effective stress in the FRP sheet*

To this aim it is expedient to define an *effective stress* in the FRP sheet, inclined to an angle β as the FRP fibres, as the mean FRP stress field $\sigma_{f,cr}(x)$ along the shear crack length $z/\sin\theta$:

$$\sigma_{fe}(\alpha) = \frac{1}{z/\sin\theta} \cdot \int_0^{z/\sin\theta} \sigma_{f,cr}[u(\alpha, x), L(x)]\, dx \tag{20}$$

which might be regarded as an equivalent constant FRP stress block along the shear crack.

For the case of S-strengthening, if one neglects the sudden stress drop between x_d and x_u, *i.e.*, if one lets $x_u \equiv x_d$, the integral (20) has a closed-form solution:

$$\sigma_{fe,S}[x_{u,S}(\alpha)] = \frac{1}{z/\sin\theta} \cdot f_{fdd} \cdot x_{u,S}(\alpha) \cdot \left[1 - k\frac{u_1}{u[x_{u,S}(\alpha)]}\right] \tag{21}$$

where the subscript *S* denotes "side bonding", $k = (1 - 2/\pi)$, f_{fdd} = debonding strength in (5), $x_{u,S}(\alpha)$ = point beyond which the sheets is fully debonded as α increases, later defined in the next section in (27), u_1 is given by (10), and $u[x_{u,S}(\alpha)]$ is the slip occurring at $x_{u,S}(\alpha)$. Note that the above equation applies when $z/(2\sin\theta) \le x_u \le z/\sin\theta$ and where $L(x_u) \ge L_e$, (that is, the second of (14)), which is always the case for S-strengthening.

For the case of U-strengthening, the integral (20) has a closed-form solution:

$$\sigma_{fe,U}[x_{u,U}(\alpha)] = f_{fdd} \cdot \left[1 - k\frac{x_{u,U}(\alpha)}{z/\sin\theta}\right] \tag{22}$$

where the subscript *U* denotes "U-jacketing", $k = (1 - 2/\pi)$, f_{fdd} is the debonding strength (5), $x_{u,U}(\alpha)$ is the point beyond which the sheets is fully debonded as α increases, later defined in the next section in (28). Note that the above equation always applies.

For the case of W-strengthening, the integral (20) does not have a closed-form solution. An approximate solution will be given in the following section.

3.6.2 *Position of the full debonding point*

In order to arrive at usable expressions for the debonding strength, an expression defining the position of the point beyond which complete debonding occurs, as function of the crack opening α, should be found. This is done by imposing:

$$u(x_u) = u_{u,cr}[L(x_u)] \tag{23}$$

To determine x_u, equation (19) is substituted into equation (23) to obtain:

$$u(x_u) = u_1 + \varepsilon_{fdd} \cdot \langle L(x_u) - L_e \rangle + u_{1,cr}(L(x_u)) \tag{24}$$

For the case of S-strengthening, as stated in the previous section, one has $z/(2\sin\theta) \le x_u \le z/\sin\theta$, $L(x_u) \ge L_e$, and $u_{1,cr}(L(x_u)) \approx 0$ (because $x_u \equiv x_d$). Thus, the FRP stress profile considered has the shape shown in Figure 7-S. Therefore, from the second of (14) one obtains:

$$u(x_{u,S}) \approx u_1 + \varepsilon_{fdd} \cdot \langle L_S(x_{u,S}) - L_e \rangle = u_1 + \varepsilon_{fdd} \cdot \left[\left(\frac{z}{\sin\beta} - x_{u,S} \cdot \frac{\sin\theta}{\sin\beta}\right) - L_e\right] \tag{25}$$

For the case of U-strengthening, from (15), one has:

$$u(x_{u,U}) \approx u_1 + \varepsilon_{fdd} \cdot \langle L_U(x_{u,U}) - L_e \rangle = u_1 + \varepsilon_{fdd} \cdot \left[x_{u,U} \cdot \frac{\sin\theta}{\sin\beta} - L_e\right] \tag{26}$$

In both cases, the expression of x_u, *i.e.*, the position of the point along the crack where full debonding occurs, as function of the crack opening α, can be explicitly obtained under the hypothesis (11).

For the case of S-strengthening, substituting (12) into (25) and solving for x_u, one has:

$$x_{u,S}(\alpha) = 2\frac{u_1 \sin\beta + \varepsilon_{fdd} \cdot (z - L_e \sin\beta)}{\alpha \sin(\theta+\beta) \cdot \sin\beta + 2\varepsilon_{fdd} \cdot \sin\theta} \tag{27}$$

For the case of S-strengthening, substituting (12) into (26) and solving for x_u, one has:

$$x_{u,U}(\alpha) = 2\frac{(u_1 - \varepsilon_{fdd} \cdot L_e) \cdot \sin\beta}{\alpha \sin(\theta+\beta) \cdot \sin\beta - 2\varepsilon_{fdd} \cdot \sin\theta} \tag{28}$$

Confirming common intuition, equations (27) and (28) indicate how the point x_u where full debonding occurs moves as the crack opens. Note that (27) only applies if $x_u \geq z/(2\sin\theta)$, while both apply where $L(x_u) \geq L_e$.
Note that in the cases of S- and U-strengthening, in the former case debonding initially takes place at the beam soffit, where the crack width is larger and the bond length is insufficient, and then gradually moves towards the crack tip. In the latter case, on the other hand, the situation is very different: at the beam soffit there is sufficient available bond length, therefore debonding occurs close to the crack tip and moves towards the crack end. By equating the derivative of (28) to zero, one obtains the point where full debonding initially occurs:

$$x_{u,U} = L_e \frac{\sin\beta}{\sin\theta} \tag{29}$$

3.6.3 *Effective debonding strength*
The maximum of the FRP effective stress, which is termed the *effective debonding strength* f_{fed}, is found by imposing:

$$\frac{d\,\sigma_{fe}[x_u(\alpha)]}{d\,\alpha} = \frac{d\,\sigma_{fe}(x_u)}{d\,x_u} \cdot \frac{d\,x_u(\alpha)}{d\,\alpha} = 0 \tag{30}$$

where the chain rule has been used. Solution of (30) allows to determine the point $x_{u,\max}$ that produces the FRP stress profile with the maximum area.
For S-strengthening, by applying (30) to (21) and noticing that $dx_{u,S}/d\alpha \neq 0$, one has:

$$\frac{d\,\sigma_{fe,S}(x_{u,S})}{d\,x_{u,S}} = \frac{1}{z/\sin\theta} \cdot f_{fdd}\left\{1 - k\frac{u_1}{u(x_{u,S})}\left[1 - x_u \cdot \frac{1}{u(x_{u,S})}\frac{d}{d\,x_{u,S}}u(x_{u,S})\right]\right\} = 0 \tag{31}$$

Substituting equation (25) into the above expression, and noticing that:

$$\frac{d}{d\,x_{u,S}}u(x_{u,S}) = -\varepsilon_{fdd} \cdot \frac{\sin\theta}{\sin\beta} \tag{32}$$

the expression of the derivative of the effective stress as function of $x_{u,S}$ is obtained, which, taken equal to zero, yields the value of $x_{u,\max,S}$ in which the maximum effective stress is realised, that is:

$$x_{u,\max,S} = \frac{z_{rid,eq} - \sqrt{k \cdot L_{eq} \cdot z_{rid,eq}}}{\sin\theta} \tag{33}$$

having let:

$$z_{rid,eq} = z_{rid} + L_{eq} \quad , \quad z_{rid} = z - L_e \cdot \sin\beta \quad , \quad L_{eq} = \frac{u_1}{\varepsilon_{fdd}} \cdot \sin\beta \tag{34}$$

where it can be noticed that: z_{rid} is equal to the beam section effective depth (which coincides with the vertical projection of the crack) minus the lower part where there is no sufficient bond length, and L_{eq} is the vertical projection of the bond length that would be necessary if the sheet had a uniform (average) strain $\varepsilon_{fdd} = f_{fdd} / E_f$.

Thus, computing (21) at the point (33), one obtains the effective debonding strength for the case of side bonding:

$$f_{fed,S} = \frac{1}{z/\sin\theta} \cdot f_{fdd} \cdot x_{u,\max,S}\left[1 - k\frac{u_1}{u(x_{u,\max,S})}\right] \tag{35}$$

where $x_{u,\max,S}$ is given by (33) and $u(x_{u,\max,S})$ is obtained from (25) as:

$$u(x_{u,\max,S}) = u_1 + \varepsilon_{fdd} \cdot \left[\left(\frac{z}{\sin\beta} - x_{u,\max,S} \cdot \frac{\sin\theta}{\sin\beta}\right) - L_e\right] \tag{36}$$

which, considering the equations (34), becomes:

$$u(x_{u,\max,S}) = u_1 \cdot \sqrt{k\frac{z_{rid,eq}}{L_{eq}}} \tag{37}$$

Replacing the previous equation into (35) with $x_{u,\max,S}$ given by (33), one gets:

$$f_{fed,S} = f_{fdd} \cdot \frac{z_{rid,eq}}{z} \cdot \left(1 - \sqrt{k\frac{L_{eq}}{z_{rid,eq}}}\right)^2 \tag{38}$$

For the case of U-strengthening, applying (30) to (22) and noticing that the maximum of (22) is found when $x_{u,U}(\alpha)$ is minimum (*i.e.*, when (29) applies), one gets:

$$f_{fed,U} = f_{fdd} \cdot \left[1 - k\frac{L_e\frac{\sin\beta}{\sin\theta}}{z/\sin\theta}\right] = f_{fdd} \cdot \left[1 - k\frac{L_e\sin\beta}{z}\right] \tag{39}$$

For the case of W-strengthening, the effective debonding strength can be expressed, with sufficient approximation, as:

$$f_{fed,W} = \frac{1}{2} f_{fu,W}(R) \tag{40}$$

where $f_{fu,W}(R)$ is the ultimate strength of the FRP strip/sheet wrapped around the corner with a radius R, given by (8).

3.7 Shear capacity with FRP

In case the reinforcement type is U or W, the Moersch resisting mechanism can be activated and the shear carried by FRP is expressed as:

$$V_{Rd,f} = 0.9\,d \cdot f_{fed} \cdot 2 \cdot t_f \cdot \left(\frac{w_f}{s_f}\right)^2 \cdot (\cot\theta + \cot\beta) \cdot \sin\beta \tag{41}$$

while for side-bonding (S) the FRP role is that of "bridging" the shear crack, so that:

$$V_{Rd,f} = 0.9\,d \cdot f_{fed} \cdot 2 \cdot t_f \cdot \frac{\sin\beta}{\sin\theta} \cdot \frac{w_f}{s_f} \tag{42}$$

with d = beam effective depth, f_{fed} = design effective strength of the FRP shear strengthening, given either by (38) for side bonding or by (39) for U-jacketing or by (40) for wrapping, t_f = thickness of FRP strip/sheet (on single side) with angle β, θ = crack angle, s_f, w_f = strip spacing and width, respectively, measured orthogonally to the fibre direction β.
Assuming cracks inclined of an angle θ=45° with respect to the vertical and strips/sheets vertically aligned at β=90°, the two previous equations become:

$$V_{Rd,f} = 0.9\,d \cdot f_{fed} \cdot 2 \cdot t_f \cdot \left(\frac{w_f}{s_f}\right)^2 \tag{43}$$

$$V_{Rd,f} = 0.9\,d \cdot f_{fed} \cdot 2\sqrt{2} \cdot t_f \cdot \frac{w_f}{s_f} \tag{44}$$

The shear verification should be performed by comparing the design acting shear with the shear capacity, given by:

$$V_{Rd} = \min\left\{ \phi V_{Rd,ct} + V_{Rd,s} + V_{Rd,f}, V_{Rd,\max} \right\} \tag{45}$$

where $V_{Rd,ct}$ is the concrete contribution, given by (*e.g.*, EC2 (CEN 1991), not accounted for):

$$V_{Rd,ct} = \frac{0.18}{\gamma_c} b_w \cdot d \cdot \min\left\{1 + \sqrt{\frac{200\text{ mm}}{d}}, 2\right\} \cdot \sqrt[3]{100 \cdot \min\{0.02, \rho_{sl}\} \cdot f_{ck}} \tag{46}$$

and $V_{Rd,s}$ is the steel contribution, given by:

$$V_{Rd,s} = 0.9\,d \cdot f_{yd} \frac{n_{st} \cdot A_{st}}{s_{st}} (\cot\theta + \cot\beta_{st}) \sin\beta_{st} \tag{47}$$

where $f_{ctd} = 0.7\,f_{ctm}/\gamma_c$ = concrete tensile strength, $\gamma_c = 1.5$ = concrete partial coefficient, b_w = web section width, ρ_{sl} = longitudinal geometric ratio, f_{ck} = concrete characteristic cylindrical strength, f_{yd} = design steel yield strength, n_{st} = transverse reinforcement arm number, A_{st}, s_{st} = area (one arm) and spacing of traverse reinforcement, e β_{st} = stirrups angle.
In (45), $V_{Rd,\max}$ is the strength of the concrete strut, given by (*e.g.*, EC2):

$$V_{Rd,\max} = 0.9d \cdot b_w \cdot \nu \cdot f_{cd} \cdot (\cot\theta + \cot\beta_{st}) / (1 + \cot^2\theta) \tag{48}$$

with $\nu = 0.6[1 - f_{ck}/250]$ (in MPa). Finally, in (45) ϕ = 1 in the absence of FRP strengthening, while ϕ = 0.5 in the presence of FRP strengthening, meaning that, when FRP reaches debonding, the concrete exploits only a fraction of its maximum strength.

4. VALIDATION OF DESIGN EQUATIONS

The results obtained with the above presented equations applied to the case of the specimen beams tested in the lab are shown in Figure 8.

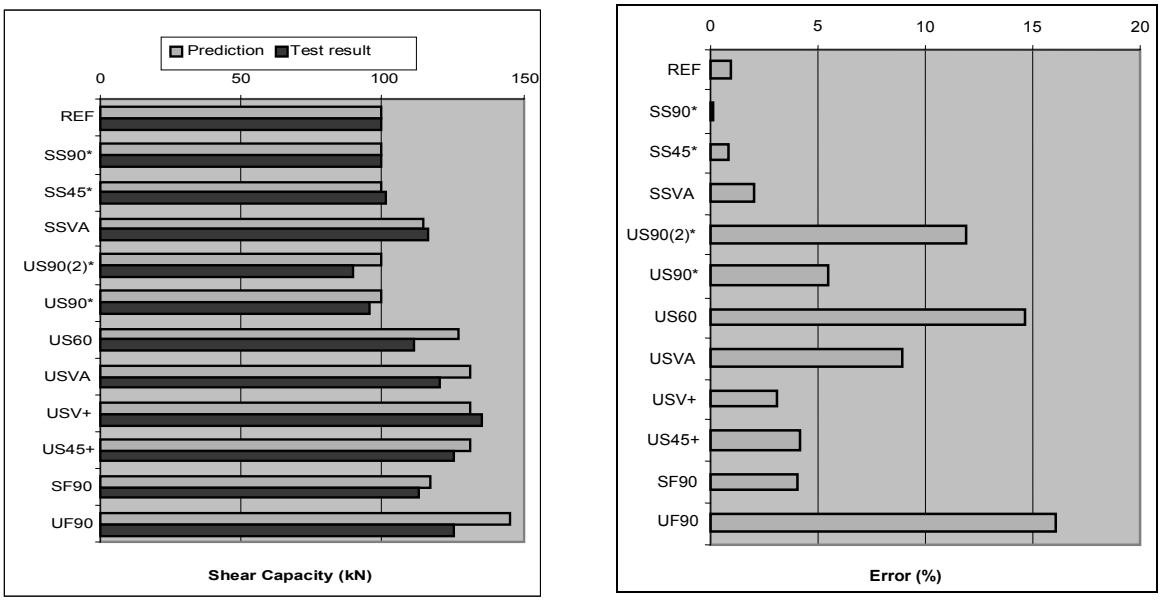

Figure 8. Prediction-test results comparison (left), and Prediction-test results error (right).

Partial coefficients were set to 1 for the prediction of experimental results, and material properties were considered with their mean values. In the equations for the variable inclination reinforcements a mean value of the strips inclinations is considered, while spacing is the effective one. The shear capacity of the reference beam was computed as the mean between the two tested unstrengthened specimens. Please note that in the specimen SS90, SS45, and US90, the contribution of FRP strengthening was not considered, as it was recognised that the diagonal shear cracks did not cross the strips.
It can be observed that the mean error on the predictions that activated the FRP strengthening is 7%, with a peak of 15% for the configurations US60 and UF90. Such an error can be considered as acceptable. Further tests are being carried out to validate the proposed equations on different reinforcing schemes.
A further information emerged from the tests regards the limitation of the strips spacing. It has been verified that the strip spacing should be sufficiently close to avoid the formation of cracks that do not cross at least one strip. From Figure 9 it can be seen that, thinking to "condensate" the strips in an "equivalent stirrup" on the strip axis, having the same height of the strip minus the effective bond length L_e from both ends in case of Side-bonding and only from one in case of U-Jacketing, shear cracks can develop that do not cross excessively spaced strips in the effective zone.

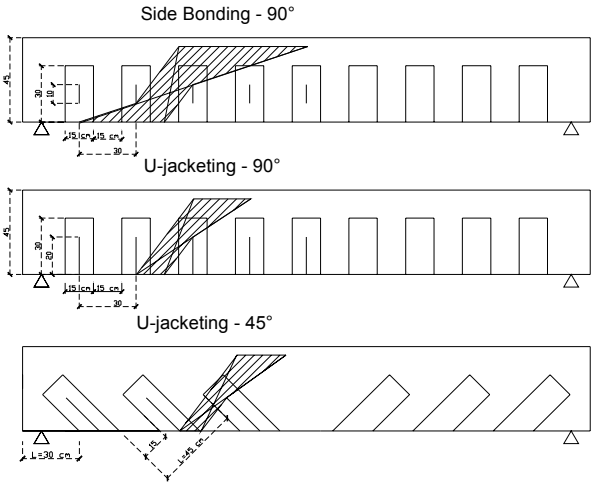

Figure 9. Crack formation fields with inadequate strip spacing.

In fact, in the case of side bonding there exists a field, shown in Figure 8, where the crack, represented in its minimum and maximum inclination, can freely pass in between strips, without crossing and activating them. From the figure, it can be seen that such field reduces its extension passing from Side-bonding to U-jacketing and increasing the fibre inclination.
This conclusion is supported by the observation of tests and from correlation of theoretical and experimental results and suggests to adopt the following limitations: in strengthening measures made with strips, these should have a width w_f, measured orthogonally to the fibres direction β, not lower than 50 mm and not larger than 250 mm, and a spacing, measured orthogonally to the fibres direction β, $s_f \le \min[0.5d,\ 3w_f,\ w_f + 200\,\text{mm}]$.

5. CONCLUSIONS

The work presented here addressed some of the still unsolved aspects in previous analytical treatments of shear strengthening of beams with composite materials (FRP) and proposes possible solutions for them. In particular, closed-form analytical expressions for the effective strength of FRP strips/sheets crossing the shear crack were found, which are then introduced in design equations for the contribution of FRP to the shear strength of RC elements. In this respect, it has been clarified that the FRP contribution to the shear strength should be computed for U and W configurations with equation (41), based on the formation of the Moersch truss, while for S configurations equation (42) should be used instead, which considers the "bridging" of cracks. Finally, it has been verified through comparison with

experimental tests that concrete cannot exploit its full contribution to the shear resistance of the beam, so that its contribution is considered with a weight ϕ=0.5 in equation (45). The equations developed showed good correlation with purposely carried out experimental tests. The equations matched the shear capacity increase with a more than acceptable error.

ACKNOWLEDGEMENTS

The authors wish to thank Interbau srl company of Milan, Italy, for the beam specimens preparation and the CFRP application.

REFERENCES

1. **Brosens, K.**, and **Van Gemert, D.** (1999). Anchorage design for externally bonded carbon fiber reinforced polymer laminates. *Proc. 4th Int. Symposium on FRP Reinforcement for Concrete Structures*, Baltimore, USA, pp. 635-645.
2. **Campione, G**., and **Miraglia, N**. (2003). "Strength and strain capacities of concrete compression members reinforced with FRP". Cement and Concrete Composites, Elsevier, 25, 31-41.
3. **CEN** (1991). Eurocode 2: Design of concrete structures – Part 1-1: General rules and rules for buildings. ENV 1992-1-1, Comité Européen de Normalisation, Brussels, Belgium.
4. ***fib*** (2001). Design and Use of Externally Bonded FRP Reinforcement (FRP EBR) for Reinforced Concrete Structures. *Bulletin no. 14, fib Task Group 9.3 'FRP Reinforcement for Concrete Structures'*.
5. **Khalifa, A., Gold, W. J., Nanni, A.** and **Aziz, A. M. I**. (1998). Contribution of externally bonded FRP to shear capacity of rc flexural members. *ASCE Journal of Composites for Construction*, **2**(4), 195-202.
6. **Monti, G., Renzelli, M.,** and **Luciani, P.** (2003). FRP Adhesion to Uncracked and Cracked Concrete Zones. *Proceedings of the 6th International Symposium on Fibre-Reinforced Polymer (FRP) Reinforcement for Concrete Structures (FRPRCS-6)*, Singapore.
7. **Monti, G., Santinelli, F.,** and **Liotta, M.A.** (2004). Shear strengthening of beams with composite materials. *Proc. 2nd International Conference on FRP Composites in Civil Engineering CICE 2004*, Adelaide, Australia, December.
8. **Täljsten B.** (1997). Strengthening of concrete structures for shear with bonded CFRP-fabrics. *Recent advances in bridge engineering, Advanced rehabilitation, durable materials, nondestructive evaluation and management*, Eds. U. Meier and R. Betti, Dübendorf, 57-64.
9. **Triantafillou, T. C.** (1998). Shear strengthening of reinforced concrete beams using epoxy-bonded FRP composites. *ACI Structural Journal*, **95**(2), March-April, 107-115.
10. **Triantafillou, T. C.** and **Antonopoulos, C. P.** (2000). Design of concrete flexural members strengthened in shear with FRP. *ASCE Journal of Composites for Construction*, **4**(4), 198-205.